International Journal of Materials Engineering and Technology

Published Online: May 2016
http://dx.doi.org/10.17654/MT015010023
Volume 15, Number 1, 2016, Pages 23-62 **ISSN: 0975-0444**

NANOLEAD-FREE SOLDER ALLOYS FOR ELECTRONIC PACKAGING AND INTEGRATION

A. E. Hammad[1,2,*] **and Sara El-Molla**[1,3]

[1]Physics Department
Faculty of Science
Zagazig University
Zagazig, Egypt
e-mail: a_hammad_82@yahoo.com
a_hammad@zu.edu.eg

[2]Basic Sciences
College of Engineering and Information Technology
University of Business and Technology
Jeddah, Saudi Arabia
e-mail: a.hammad@ubt.edu.sa

[3]Institute for Nanoelectronics
Technische Universität München
München, Germany
e-mail: sara.el-molla@tum.de
sara.el-molla@nano.ei.tum.de

Abstract

Synthesis of metal nanoparticles with specific properties is a newly established research area attracting a great deal of attention. Several methods have been put forward for synthesis of these materials,

Received: October 23, 2015; Accepted: November 22, 2015
Keywords and phrases: nanolead-free solders, alloy, melting temperature, wettability, mechanical properties, microstructure.
*Corresponding author

namely chemical vapor condensation, arc discharge, hydrogen plasma-metal reaction, and laser pyrolysis in the vapor phase, microemulsion, hydrothermal, sol-gel, sonochemical. Nanoscale lead-free solders (i.e., Sn-*x*Ag [$x = 0, 20, 40, 60, 80, 100$(wt%)], Sn-3.0Ag-0.5Cu, Sn-3.5Ag-0.5Cu, Sn-3.5Ag-*x*Zn ($x = 0.5$ to 3.5wt%) and Sn-0.7Cu) have been investigated. For Sn-3.5Ag and Sn-3.5Ag-0.5Cu nanoparticles, the melting temperature with average size of 30 nm was 210°C and 201°C, much lower than that of bulk alloy. Also, Sn-Ag-Cu nanopowders showed good wettability with contact angles less than 30°. The peak melting temperatures of the 21 nm, 18 nm and 14 nm Sn-0.7Cu nanoparticles were 212.9°C, 207.9°C and 205.2°C, respectively. In this paper, the fundamentals of synthesis of nanolead-free solder materials including their characterization and their use in microelectronic packaging are reviewed.

1. Introduction

Nanoscience and nanotechnology involve the design, fabrication, and engineering of materials and systems at the nanometer scale (1-100 nm). Materials and systems at this scale may exhibit novel mechanical, electronic, electrical, magnetic, and optical properties. There have been significant developments in new nanomaterials fabrication and novel nanotechnology development, e.g., the emerging and evolving of carbon nanotubes, nanoparticles, and nanowires [1-3].

Today, solders are used in numerous applications and in electronics industry for connecting electrical components. Soldering is a well-known metallurgical joining method using a filler metal (the solder) [4]. Material selections for solder alloys are thus critical and play key roles in joint reliability of assemblies in electronic packaging. Over the past several decades, Pb-Sn systems have been the mainstay of the conventional solder process owing to their unique combination of material properties such as good wettability, low cost, high ductility, and low eutectic temperature [5].

2. Lead-bearing Solders

The Sn-Pb solder is the most widely utilized soldering alloy, the

popularity of this alloy is due to its relatively low melting temperature, aggressive bonding characteristics, good electrical continuity, and low cost [6, 7].

Lead-bearing solders, particularly the eutectic 63Sn-37Pb or near-eutectic 60Sn-40Pb alloys, have been used extensively in interconnection technologies such as pin through hole (PTH), ball grid array (BGA), surface mount techniques (SMT), chip scale packaging (CSP), flip-chip, etc. [8], where strict electrical, mechanical and thermal properties of solder alloys are essential (Figure 1).

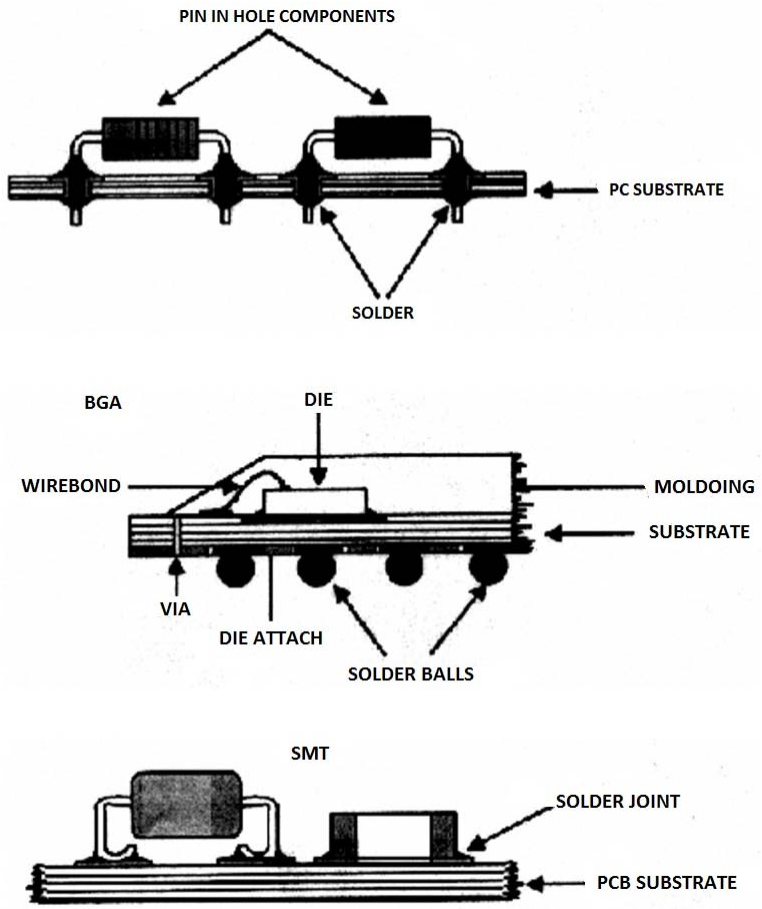

Figure 1. Schematic structures of PTH, SMT and BGA packages using solder interconnects.

3. Health and Environmental Concerns

Medical studies have shown that Pb is a heavy metal toxin that can damage the kidney, liver, blood and the central nervous system. In Europe, the elimination of Pb in solder alloys has gained a common consensus. From January, 2004, European nations will adopt Pb-free solder alloys in all electronic assemblies, according to Directive on Waste from Electrical and Electronic Equipment (WEEE) [7].

Recycling lead in electronics can increase the cost and efforts than that in batteries or cathode ray tubes (CRT) due to the difficulty in removing it from the components of electronic products. Therefore, rapid switching and great effort for seeking Pb-free solder alloys as a replacement for Sn-Pb eutectic alloy [5].

4. Lead-free Solder Alloys

Basic criteria were proposed for ‘‘perfect’’ lead-free alternatives. The most important characteristics that must be considered in selecting suitable lead-free solders are nontoxic, availability, low melting temperature, low cost, good wettability, better electrical properties, and adequate mechanical properties [7]. Table 1 summarizes some of important properties of solder alloys [7].

Table 1. Important properties of solder alloys

Properties relevant to reliability and performance	**Properties and Aspects relevant to manufacturing**
Electrical conductivity	Melting/liquidus temperature
Thermal conductivity	Wettability to copper
Coefficient of thermal expansion	Cost
Shear properties	Environmental friendliness
Tensile properties	Availability and number of suppliers
Creep resistance	Manufacturability using current processes
Fatigue properties	Ability to be made into balls
Corrosion and oxidation resistance	Copper pick-up rate
Intermetallic compound formation	Recyclability
	Ability to be made into paste

Up to now, several types of binary and ternary Sn-based lead-free solders such as Sn-Zn, Sn-Ag, Sn-Cu, Sn-Ag-Zn and Sn-Ag-Cu have been studied [9, 10]. Table 2 shows major lead-free solder system candidates to replace eutectic Sn-Pb.

Table 2. Listing of major lead-free solder system candidates to replace eutectic Sn-Pb

Solder	Weight Percent								Temperature (°C)		
	Sn	In	Ag	Sb	Bi	Cu	Au	Zn	Liquidus	Solidus	Range
60Sn-40Bi	60				40				170	138	32
50Sn-50In	50	50							125	118	7
91Sn-9Zn	91							9	199	Eutectic	0
96.5Sn-3.5Ag	96.5		3.5						221	Eutectic	0
97Sn-3Cu	97					3			300	227	73
80Au-20Sn	20						80		280	Eutectic	0
95Sn-5Sb	95			5					240	235	5
83.6Sn-8.8In-7.6Zn	83.6	8.8						7.6	187	181	6
98Sn-1.5Ag-0.5Cu	98		1.5			0.5			210	215	5
54.0Bi-29.7In-16.3Sn	16.3	29.7			54				81	Eutectic	0
65Sn-25Ag-10Sb	65		25	10					233	Eutectic	0
95.5Sn-4Cu-0.5Ag	95.5		0.5			4			260	204	65

5. Nanosolder for Electronics Interconnect Applications

Recently, as micro-/nano-systems technologies are advancing, the size of electrical components is shrinking leading to an increase in the number of input/output terminals (Figure 2) [7].

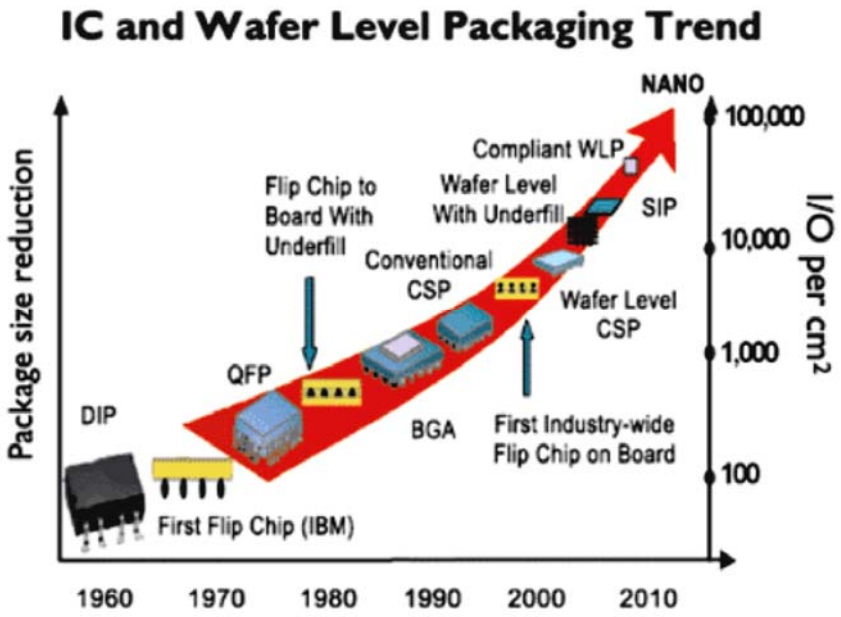

Figure 2. IC and wafer level packaging trend.

Among the many novel lead-free solders, nanocomposite solders are considered the most probable candidates to replace current lead-free solder. For example, researchers examined the influence of reinforcing TiO_2 and Al_2O_3 nanoparticles on the microstructural development and hardness of eutectic Sn-Ag-Cu solders, and measurements of the microhardness, ultimate tensile strength (UTS) and 0.2% offset yield strength (0.2YS) revealed that the addition of TiO_2 and Al_2O_3 nanoparticles enhanced the overall strength of the eutectic solder. Carbon nanotubes (CNTs) were introduced into the solder matrix. The resulting solder exhibited a lower diffusion coefficient, which signified that the presence of CNTs was effective in retarding the growth of the IMC layer [11].

High melting point, in turn, pushes the solder reflow (i.e., spreading of molten alloy on the contact surface) temperature to over 260°C and severely limits the applicability of this metal alloy to temperature sensitive components and/or low cost organic printed circuit boards. It was found that decreasing the size of the material could reduce its melting point [12]. The

size-dependent nature of melting nanoscaled metal particles has received attention from a number of experimental studies. A well accepted model for the melting temperature T^*_{melt} is given by the Gibbs-Thomson formula

$$T^*_{melt} = T^*_{bulk}\left(1 - \frac{w}{R^*}\right), \tag{1}$$

$$w = \frac{2\sigma^*}{\rho_s L}, \tag{2}$$

where R^* is the radius of the spherical particle and T^*_{bulk} is the bulk melting temperature, which is the temperature at which the material would melt if the interface was flat. The physical constants ρ_s, L and σ^* are, respectively, the density of the material in the solid phase, the latent heat of fusion, and a parameter proportional to surface energy effects acting on the solid-melt interface.

The effect of equation (1) is that for small R^*, the melting temperature of the spherical particle is significantly reduced. This size dependence on melting temperature is a consequence of nanoparticles having a much larger surface-to-volume ratio than bulk materials, and occurs for both for round and facetted particles. Since both the solid and liquid molecules on a curved surface are more weakly bonded than their counterparts in the solid and liquid bulk, the difference between the binding of liquid and solid molecules on the surface is a driving factor for this reduced melting temperature. Thus, ultimately the size dependence on melting temperature of a nanoscaled spherical particle is due to the very high surface-to-volume ratio and lower interfacial energy of the liquid phase. We note that there is no observable reduction in melting temperature for macrosized particles; this is a small-scale phenomenon only, as the length scale ω in equation (1) is typically of the order of nanometres. The constant σ^* in equation (2) is a measure of the surface energy effects, also referred to as surface tension.

Nanoparticles have gained increasing attention in recent years owing to the large surface to volume ratio and quantum size effect. Therefore, there is

an increasing interest in the application of nanoscale metal alloys as low temperature lead-free solders. Due to the environmental concern against the lead component of the eutectic Sn-Pb solders, electrically conductive adhesives (ECAs) have been explored for surface mount technology and flip chip application as lead-free alternatives. ECAs are composites of the polymer and metal fillers. Among the metal fillers, silver may be used because silver has the highest electrical conductivity and its oxides are also conductors [13]. Tin has been proposed as alternative conductive filler. The synthesis of a nanosize binary Sn-Ag alloy of specific composition is much more difficult than that of monocrystalline nanotin and nanosilver particles [14].

6. Methods for Synthesis of Nanostructured Metals

There are many methods to produce nanoparticles, such as chemical vapor deposition CVD [15, 16], laser ablation [17, 18], microemulsion [19, 20], sol-gel [21, 22], and chemical reduction [23, 24]. In addition, there are two general approaches top-down and bottom-up to the synthesis of nanomaterials and the fabrication of nanostructures. The principle behind the top-down approach is to take a bulk piece of the material and then modify it into the wanted nanostructure and subsequent stabilization of the resulting nanosized metal nanoparticles by the addition of colloidal protecting agents. Cutting, grinding and etching are typical fabrication techniques, which have been developed to work on the nanoscale. The sizes of the nanostructures which can be produced with top-down techniques are between 10 to 100 nm. Bottom-up self-assembly refers to construction of a structure atom-by-atom, molecule-by-molecule or cluster-by-cluster. Colloidal dispersion used in the synthesis of nanoparticles is a good example of a bottom-up approach. An advantage of the bottom-up approach is the better possibilities to obtain nanostructures with less defects and more homogeneous chemical compositions. Table 3 shows difference between top-down and bottom-up approaches.

Table 3. Top-down and bottom-up approaches to synthesis nanomaterials and the fabrication nanostructures

Approach	Top-down	Bottom-up
Principle	These approaches use larger (macroscopic) initial structures, which can be externally-controlled in the processing of nanostructures.	- These approaches include the miniaturization of materials components (up to atomic level) with further self-assembly process leading to the formation of nanostructures. - During self-assembly the physical forces operating at nanoscale are used to combine basic units into larger stable structures.
Examples	Typical examples are etching through the mask, ball milling, and application of severe plastic deformation.	Typical examples are quantum dot formation during epitaxial growth and formation of nanoparticles from colloidal dispersion.
Cost	By nature, are not cheap and quick to manufacture.	Fabrication is much less expensive.
Drawback	Introduces internal stress, surface defects (i.e. imperfections) contaminations.	Less defects, homogeneous chemical composition. Better short and long range ordering.

Most of these synthesis techniques are faced with some problems when being scaled up for industrial application. The CVD and laser ablation methods have problems related to high-temperature processing, high cost, and low production efficiency. The microemulsion and sol-gel methods with organic solvents also exhibit some problems, such as pollution of the environment and impurity. The laser vaporization can be used to synthesize clean nanoparticles and nanoalloys but the technique suffers from large size distributions and low yields. For these reasons, these techniques are not desirable. Among these, chemical reduction is the most suitable method for industrial manufacture. It is a low-temperature process with relatively low production cost and high yield. Furthermore, compositions of the nanoparticles prepared by this method can be precisely controlled by carefully adjusting the synthesis parameters, such as pH value and temperature [25].

7. Synthesis and Characterization of Lead-free Nanosolder Alloys

Pande et al. [12] prepared Sn-Ag nanoalloy via two fundamentally differing routes.

Route 1. The Sn-Ag nanoalloy was prepared following a two-step procedure. In the first step, 40 mL of silicone oil, 1 g of hydrazine hydrate, and 96.5 mg of 99.9% tin powder were mixed together in a 100 mL two necked flask equipped with stirring and refluxing equipment. The mixture was heated to ~240°C with vigorous stirring for 3 h for molecularization of metallic tin. In the second step, 3.5 mg of black resorcinol capped silver nanoparticles was added into the flask but at room temperature. Alternatively, oleic acid capped silver nanoparticles were used, which yield similar result. The reaction mixture containing molecularized tin and silver nanoparticles was then heated to ~240°C for 8 h reflux. The reaction mixture was cooled, and the suspended particles were centrifuged to obtain the black product. Finally, the black mass was washed thrice with petroleum ether (60-80) and three times with tetrahydrofuran (THF) and then dried under vacuum. The percent yield was 87%.

Route 2. In this step, 20 mL of silicone oil, 20 mL of ethylene glycol, 96.5 mg of 99.9% Sn(II) acetate, 3.5 mg of 99.9% Ag(I) acetate, and 200 mg of NaOH were mixed in a 100 mL two necked flask. The mixture was then sonicated (~2 h) for homogeneous mixing. The mixture turned black. After that, the mixture was heated to ~240°C with vigorous stirring for 8 h for the preparation of Sn-Ag nanoalloy. Next, the reaction mixture was cooled, and the suspended particles were centrifuged to obtain the black product. Finally, the black mass was washed with petroleum ether (60-80) and THF. The product yield was 93%.

Sn-Ag nanoparticles can be obtained with different size distributions by changing the stirring forces as well as the sonication time. The wettability of eutectic Sn-Ag alloy on stainless steel happens to be much higher (contact angle 18.0°) than that on a copper surface (contact angle 14.0°). Very interestingly, the nanopowder shows a melting point as low as 128°C.

One of the interesting observations in case of Route 2 is that, when tin acetate and silver acetate (96.5:3.5) are heated in ethylene glycol (pH ~11-12) under refluxing conditions, no alloy resulted and instead Sn(II) glycolate and silver nanoparticles in dispersion are obtained. However, when tin acetate and silver acetate are dispersed in silicone oil and treated with ethylene glycol (pH ~11-12) at room temperature and refluxed at ~240°C (~4 h) followed by sonication (~2 h), a black colored alloy is obtained. Hence, silicone oil plays an important role in the alloy formation in the presence of ethylene glycol. In this procedure, the particles become quite smaller (~30 nm) than the particles obtained from Route 1. This size reduction is due to the sonication effect before refluxing. The effect of sonication on the mean particle size has been investigated. Sonication produced a drastic particle-size reduction, and the particle size relates to the melting point. The particle size drastically decreased to 30 ± 5 nm. The thermal analysis of the Sn-Ag nanoalloy of the smaller size particles (~30 nm) exhibits a drastic change in the endothermic peak position (~128°C) with the decrease in particle size indicating a sharp lowering of the melting point (~128°C).

Zhang et al. [26] synthesized nanoparticles of lead-free solder alloys (Sn-3.5Ag (wt%) and Sn-3.0Ag-0.5Cu (wt%)) through a chemical reduction method by using anhydrous ethanol (CH_3CH_2OH), 1,10-phenanthroline ($C_{12}H_8N_2 \cdot H_2O$) and sodium borohydride ($NaBH_4$) as the solvent, surfactant and reducing agent, respectively. Tin (II) 2-ethylhexanoate ($C_{16}H_{30}O_4Sn$) and silver nitrate ($AgNO_3$) were used. In terms of the synthesis of Sn-3.0Ag-0.5Cu nanoparticles, copper (II) ethoxide monohydrate ($Cu(OC_2H_5)_2 \cdot H_2O$) was added to the reactant.

In a typical synthesis of Sn-3.5Ag nanoparticles, 0.2998g of tin (II) 2-ethylhexanoate, 0.0051g of silver nitrate, and 0.2775g of 1,10-phenanthroline were mixed with 60 mL of anhydrous ethanol to prepare the precursor solution. The mixture was stirred for about 2 hours before 0.1892 g of sodium borohydride was added into the stirring solution. The reaction time was the variable to be tested in the experimental procedure, so set reaction times of 15, 30, 45, and 60 min were used. The as-synthesized nanoparticles were

precipitated by a centrifuge at a rate of 4000 rpm for 45 min. Due to the low solubility of $NaBH_4$ in ethanol, the reaction rate during the separation process was extremely low. The reduction reaction could be stopped at any predetermined time through this method. The nanoparticles obtained were rinsed 3 times with anhydrous ethanol and then dried in the vacuum chamber at 40°C for 8 hours. The synthesis procedure of Sn-3.0Ag-0.5Cu nanoparticles was similar to that of Sn-3.5Ag nanoparticles.

Most of the Ag and Cu cations were reduced to their metallic form and formed nuclei, respectively. At the same time, a few Sn atoms were generated in the solution. With mechanical agitation, the nuclei of Ag and Cu acted as the heterogeneous seed, absorbed Sn atoms and formed the intermetallic phases, Ag_3Sn and Cu_6Sn_5.

The rest of the Sn atoms, that were not used in the formation process of the intermetallic phases could nucleate and grew into the Sn phase. The capping effect of the surfactant and the size of the synthesized nanoparticles can be well controlled. The formation process of SAC nanoparticles was illustrated in Figure 3 [26]. A typical SEM image of the SAC nanoparticles synthesized at room temperature with a reaction time of 60 min was shown in Figure 4 [26]. The particles were basically spherical with a narrowdiameter distribution of 37.6 ± 14.9 nm. Despite the low content of Cu in the core-shell structure, the relatively small particle size could make it detectable.

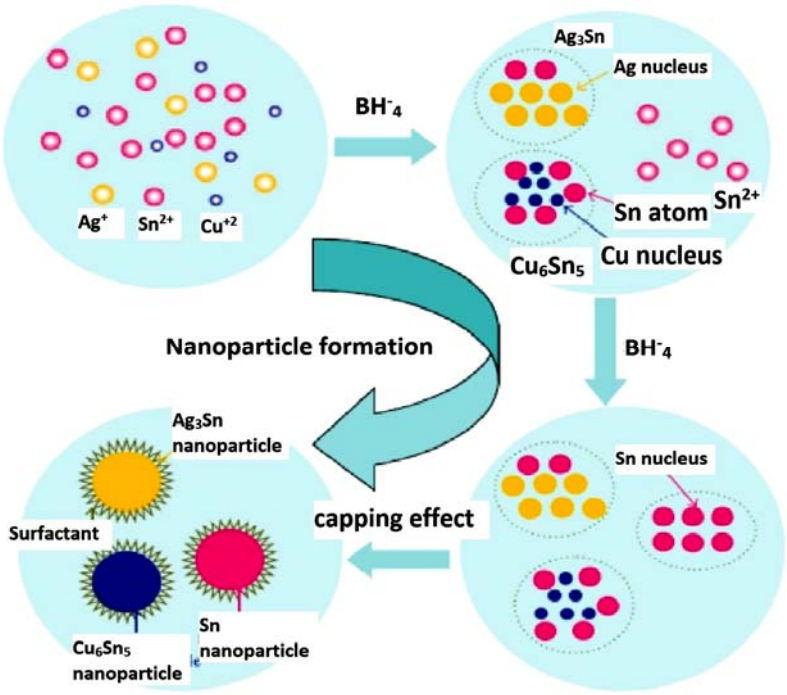

Figure 3. The formation process of Sn-3.0Ag-0.5Cu nanoparticles.

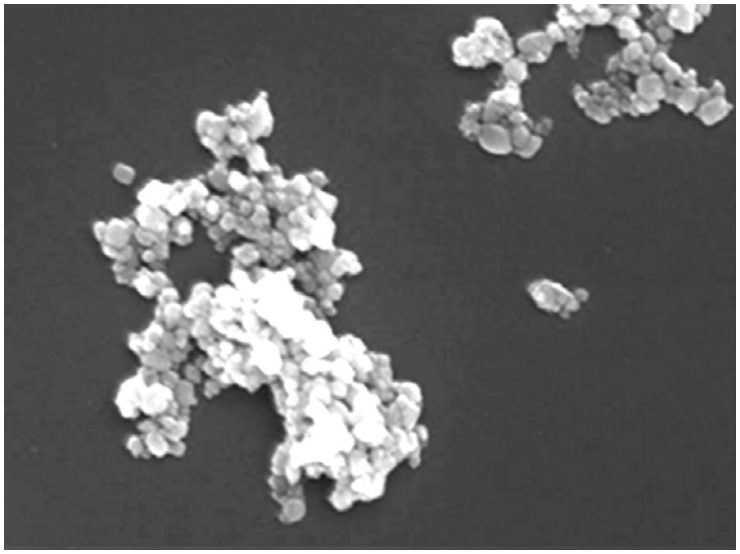

Figure 4. Typical SEM image of the synthesized SAC nanoparticles with a reaction time of 60 min [26].

Zou et al. synthesized tin nanoparticles with different size distribution using chemical reduction method by applying $NaBH_4$ as reduction agent [27]. In different cases, different amounts of surfactant, 0, 0.1, 0.2, and 0.4 g, were chosen to control the morphology and size distribution of the products.

The Sn nanoparticles synthesized using 0.33 g of tin(II) 2-ethylhexanoate as precursor in the presence of 0, 0.1, 0.2 and 0.4 g surfactants were marked as Sn1, Sn2, Sn3 and Sn4, respectively. The melting temperatures of the Sn1, Sn2, Sn3 and Sn4 nanoparticles in diameter of 81, 40, 36 and 34 nm were 226.1, 221.8, 221.1 and 219.5°C, and the corresponding latent heats of fusion were 35.9, 23.5, 20.1 and 15.6 J/g, respectively.

Using the same route, Jiang et al. synthesized tin nanoparticles with various sizes by using 2.1×10^{-4} mol tin(II) acetate as a precursor in the presence of 0.045 mol surfactants and 0.1 g sodium borohydride as reducing agents [28]. The average particle size calculated was around 61 nm. The interplanar spacing was about 0.29 nm which corresponds to the orientation of (200) atomic planes of the tetragonal structure of Sn.

The average particle size of Sn nanoparticles which were synthesized by using 4.2×10^{-4} mol tin(II) acetate as a precursor in the presence of 0.045 mol surfactants was around 52 nm. The melting point of the Sn nanoparticles was around 228.0°C, which was 4°C lower than that of micron sized Sn particles. The average particle size of Sn nanoparticles which were synthesized by using 1.1×10^{-3} mol tin(II) acetate as a precursor in the presence of 0.045 mol surfactants was around 85 nm. The melting point of the as-synthesized Sn nanoparticles was 231.8°C, which was still lower than the melting point of micron sized Sn particles.

The average particle size of Sn nanoparticles which were synthesized by using 1.75×10^{-4} mol tin(II) acetate as a precursor in the presence of 0.045 mol surfactants was around 26 nm. The melting point of these particles was around 214.9°C, which was 17.7°C lower than that of micron sized Sn particles. The heat of fusion of the as-synthesized Sn nanoparticles was smaller than that of micron sized Sn powders.

Zhang et al. prepared successfully Sn-3.0Ag-0.5Cu (mass fraction, %) alloy nanoparticles [29]. In different conditions, different amounts of tin(II) 2-ethylhexanoate were mixed into 60 mL anhydrous ethanol and the concentrations for SAC1, SAC2, SAC3, SAC4 were 0.0068, 0.0101, 0.0202 and 0.0271 mol/L, respectively. In a typical synthesis process, for example SAC1, 0.222 g surfactant was added into the solution and intensively stirred for about 2h in atmospheric environment. Afterwards 0.0946g reducing agent was added into the homogeneous precursor solution and stirred for another 1h till the end of the reaction.

The particle sizes of SAC1 and SAC2, whose solution concentrations were at relatively low level, were smaller than 50nm and mainly concentrated in the range of 15-40 nm. In the case of higher reactant concentration, namely SAC3 and SAC4, the proportion of particles less than 50 nm was rapidly reduced to about 65%. Despite the average diameters for SAC3 and SAC4 were almost the same, the size distribution of the latter was much larger due to the thicker reactant. It should be noticed that there were even particles of about 200 nm in the SAC4 sample. In addition, the particle sizes of SAC1 and SAC2 were well controlled considering the lower level of surfactant concentration. That is to say, the particle size was mainly influenced by the reactant concentration [29].

Nanoparticles of Sn-3.0Ag-0.5Cu were also synthesized using the same method by Zou et al. [30]. Authors mixed 0.3293 g tin(II) 2-ethylhexanoate, 0.0047 g silver nitrate, 0.0017 g copper(II) acetate monohydrate and 0.1110 g 1,10-phenanthroline into a 60 mL anhydrous ethanol solution. The solution was then stirred intensively for 2 h. Then 0.1892 g sodium borohydride was added into the solution and the reaction continued for 1 h at ambient temperature. Different amounts of surfactant, i.e. 0.1110 g, 0.4440 g, and 0.8880 g, were chosen to control the morphology and size distribution of the products.

The results showed that the calorimetric onset melting temperature of the Sn-3.0Ag-0.5Cu alloy nanoparticles could be as low as 200°C, which was about 17°C lower than that of the bulk alloy (217°C). The images of the as-

prepared nanoparticles indicated that the major particle size of Sn-3.0Ag-0.5Cu nanoparticles is smaller than 50 nm [30].

As well, Zou et al. synthesized Sn-3.5Ag nanoparticles [31]. They selected different amounts of surfactant, i.e. 0, 0.15, 0.3, and 0.6. It was found that the larger ratio of the weight of the surfactant to the precursor was used, the smaller the particle size was obtained. This is due to the capping effect caused by the surfactant molecules coordinate with the nanoclusters, and resultantly a larger amount of surfactant restrict the growth of the nanoparticles. Figure 5 shows the typical SEM images of the as-synthesized Sn3.5Ag nanoparticles: (a) surfactant 0; (b) surfactant 0.15; (c) surfactant 0.3; (d) surfactant 0.6. The particle size distribution of Sn-Ag with sample surfactant 0 was very large, from 30 to 1,500 nm. The particle size distribution of sample of surfactant 0.15 was much smaller than sample with surfactant 0, from 20 to 300 nm. The particles size distribution of Sn-Ag sample with surfactant 0.3 had the similar size distribution as Sn-Ag sample with surfactant 0.15, from 20 to 300 nm. The particle size distribution of Sn-Ag sample with surfactant 0.6 was even smaller than Sn-Ag sample with surfactant 0.3, from 10 to 150 nm, and most of the particles were smaller than 100 nm.

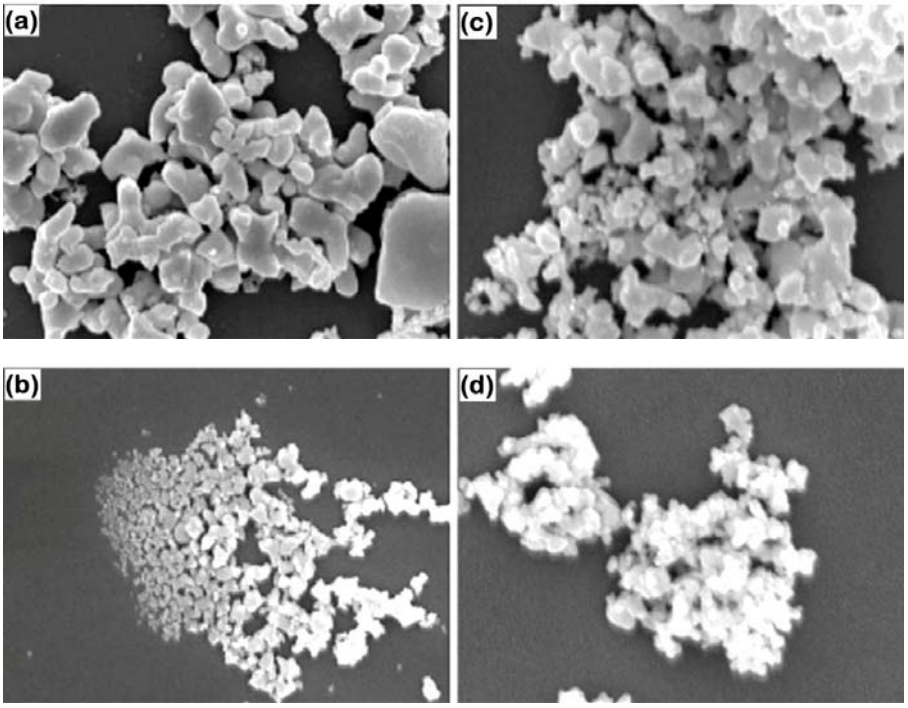

Figure 5. The SEM images of Sn3.5Ag nanoparticles with different amounts of surfactant, i.e. (a) 0, (b) 0.15, (c) 0.3, and (d) 0.6 [31].

In addition, the larger depression of the melting temperature of the nanoparticle with 50 nm was about 7°C. It is deemed that the equilibrium melting temperature of Sn-3.5Ag bulk alloy was 221°C. The calculated results show that when the size of the nanoparticles decreases to be 100 nm, the melting temperature will decrease dramatically. Due to the oxidation and size-dependent properties of the latent heat of melting, the latent heat of melting of Sn-3.5Ag nanoparticles was much smaller than that of the bulk alloy.

Jo et al. synthesized low-cost, highly conductive Sn-*x*Ag [x = 0, 20, 40, 60, 80, 100(wt%)] bimetallic nanoparticles for inkjet printing, using a polyol process with poly(vinyl pyrrolidone) PVP (MW = 55,000) and $NaBH_4$ as the surface stabilizer and the reducing agent, respectively [32]. Surface oxidation layer was observed on the Sn nanoparticles for both the 40Ag-60Sn and

20Ag-80Sn nanoparticles. The TEM analysis, on the other hand, reveals no surface oxidation layer for the 80Ag-20Sn and 60Ag-40Sn nanoparticles.

The results of XRD analysis show that the 100Sn, 100Ag, 40Ag-60Sn, and 20Ag-80Sn compositions have β-Sn, fcc, β-Sn+Ag_3Sn, and β-Sn+Ag_3Sn phases, respectively. For the 20Ag-80Sn nanoparticles, a portion of the β-Sn phase was much higher than that of the 40Ag-60Sn nanoparticles. Hence, a large amount of surface oxidation layer was observed in the 20Ag-80Sn nanoparticles. In contrast to the TEM images, the XRD analysis of the 20Ag-80Sn nanoparticles shows no SnO_x peak, because the XRD analysis failed to detect the thin surface oxidation layer.

The results of analyses confirm that the formation of a bimetallic phase, such as Ag_4Sn or Ag_3Sn, hinders the β-Sn phase and, consequently, leads to the removal of the surface oxidation layer. The sheet resistance is decreased by the conductive Sn-Ag phases, such as the fcc, Ag_4Sn, and Ag_3Sn phases, but sharply increased by the low-conductive Sn nanoparticles and the surface oxidation layer on the Sn nanoparticles. An increase in the solubility limit of Sn in Ag enables fcc and $Ag_4Sn + Ag_{6.7}Sn$ phases to be observed in 80Ag-20Sn and 60Ag-40Sn compositions; however, these phases are inconsistent with the expected phases of the bulk phase diagram. In the 40Ag-60Sn and 20Ag-80Sn nanoparticles, the β-Sn and Ag_3Sn phases were observed in accordance with the bulk phase diagram. The β-Sn phase renders the surface oxidation layer observable in both compositions but to a much greater extent in the 20Ag-80Sn nanoparticles than in the 40Ag-60Sn nanoparticles. The sheet resistance results confirm that 80Ag-20Sn and 60Ag-40Sn bimetallic nanoparticles are suitable candidates for inkjet printing materials [32].

Pan et al. [33] synthesized Sn-3.5Ag alloy nanosolders by using different amounts of reducing agent ($NaBH_4$). The experimental results revealed that increased addition of $NaBH_4$ to the bath (0.01-1 g) transformed the color of the precipitate from grey to black. It might be attributed to the fact that the reduction reaction was incomplete because of the insufficient amount of reducing agent. For the reduction reaction to be completed, it is essential to keep the reducing agent amount of at least 0.1 g in this system.

As nanoparticles tend to agglomerate together in the SEM images, thus PVP plays an important role in the successful synthesis of the Sn-3.5Ag alloy nanoparticles. SEM image for Sn-3.5Ag solder alloy obtained without PVP demonstrated that most of the Sn-Ag nanoparticles aggregated into a cluster. Increased addition of PVP (0.2 g) resulted in stronger aggregation of primary particles. Nevertheless, further increase in the PVP content to 2 g significantly decreased the agglomeration of nanoparticles and greater dispersion of nanoparticles was noticed. The dispersion of the nanoparticles in the presence of PVP could be attributed to the fact that the protective polymer PVP adsorbed on the nanoparticles and exhibited protective function by steric stabilization. The other part of the protective polymer dissolved in the free-state in the suspension of the alloy nanoparticles as a free polymer.

X-ray diffraction (XRD) patterns revealed that Ag_3Sn was formed due to the successful alloying process. The morphology of Sn-3.5Ag alloy nanosolder changed with increase in the PVP content in the bath. The size of the nanoparticles ranged from 300 to 700 nm.

Sn-Ag alloy nanoparticles were synthesized and their thermal properties were studied [34]. The melting point can be achieved as low as 194°C when the diameter of the nanoparticles is around 10 nm. The 64 nm (average diameter) Sn-Ag alloy nanoparticle pastes showed good wetting properties on the cleaned copper foil surface and the IMCs formed. Figure 6(a) shows the TGA curve of the dried Sn-Ag alloy nanoparticles in nitrogen atmosphere. The weight loss below 180°C might be due to the evaporation of a small amount of absorbed moisture and surfactants. Above 180°C, the weight gain was observed, which was attributed to thermal oxidation of the Sn-Ag alloy nanoparticles. Figure 6(b) displays the thermal profile of the dried Sn-Ag alloy nanoparticles. The melting point of the Sn-Ag nanoparticles was found at 209.5°C, about 13°C lower than that of the micrometersized 96.5Sn-3.5Ag particles (222.6°C).

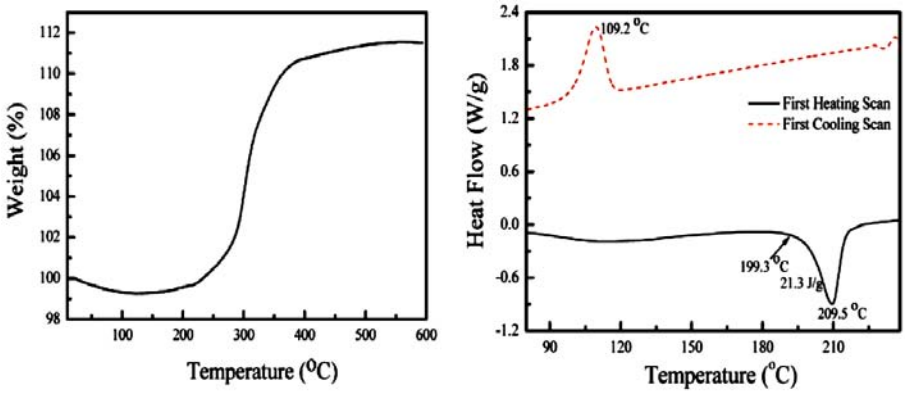

(a) (b)

Figure 6. TGA (a) and DSC (b) curves of the Sn-Ag alloy nanoparticles which were synthesized by using 7.4×10^{-4} mol of tin(II) 2-ethylhexanoate and 3.0×10^{-5} mol of silver nitrate as precursors in the presence of 5.6×10^{-4} mol of surfactants [34].

Zou focused on the research aimed to lower the melting temperature of the lead-free solder alloy through decreasing the particle size down to nanometer level by chemical reduction method [35]. The Sn-3.5Ag and Sn-3.5Ag-0.5Cu nanoparticles (average size about 30 nm) are obtained by adjusting the drops rate of reductant, the concentration of surfactant and reactant. It was found that when the addition rate of reductant is decreased, the particle sizes and size distribution showed the same result. Also, the melting temperature of lead-free solder showed strong size-dependent tendency and the melting temperature of Sn-3.5Ag and Sn-3.5Ag-0.5Cu nanoparticles with average size of 30 nm was 210°C and 201°C, much lower than that of bulk alloy.

An attempt was made to synthesize Sn-3.5Ag-xZn (x = 0.5 to 3.5 wt%) alloy nanoparticles by Lin et al. [36]. The chemical precipitation was carried out by using $NaBH_4$ as a reducing agent and PVP as a stabilizer. X-ray diffraction patterns revealed that Ag_3Sn was formed due to the successful alloying process. Other IMCs such as Ag_4Sn and Ag_5Zn_8 were also obtained in the XRD patterns. Results on TEM revealed that the isolated particles

were spherical in shape and the particle size varied from 2 to 10 nm. The microstructure for Sn-3.5Ag-0.5Zn alloys showed selected area diffraction patterns for Ag_3Sn nanoparticles. However, diffraction patterns for compounds like Ag_4Sn and Ag_5Zn_8 could not be obtained due to the strong aggregation of nanoparticles. The morphology of Sn-Ag-Zn nanoparticles revealed that the major particle size of Sn-Ag-Zn nanoparticles were in the range of 60-80 nm.

Sn-3.0Ag-0.5Cu nanoparticles with different size distribution could be successfully synthesized using different amounts of surfactant i.e. 0.075 g, 0.15 g, 0.3 g and 0.6 g, which were also used to prevent the synthesized nanoparticles from aggregating and being oxidized [37]. The experimental results indicated that the major particle size of Sn-3.0Ag-0.5Cu nanoparticles was smaller than 100 nm. It was evidenced by the differential scanning calorimetry curves that the melting temperature of Sn-3.0Ag-0.5Cu nanoparticles was 214.7°C, 213.8°C, 213.5°C and 213.6°C lower than that 217.8°C of the bulk alloy. In addition, the undercooling of the Sn-3.0Ag-0.5Cu nanoparticles was in the range of 82.0-88.5°C at different cooling rates, which was much larger than that of the Sn-3.0Ag-0.5Cu micro-sized particles, showing stronger cooling rate dependence.

Sn-3.0Ag-0.5Cu nanosolders were produced via a chemical reduction method by Yung et al. [38]. Tin sulfate ($SnSO_4$), silver nitrate ($AgNO_3$), copper nitrate ($Cu(NO_3)_2 \cdot 2.5H_2O$), PVP (Mw = 40,000 g/mol), and $NaBH_4$ were used as precursors, surfactant, and reducing agent, respectively.

Through different reaction conditions including variation of the amounts of PVP and $NaBH_4$, temperature, and pH value, the nanosolder particle diameter was well controlled to the range of 10 nm to 22 nm, and the size-dependent melting point was depressed to 204.4°C. Although Sn oxides formed on the nanosolders during the reduction process, these oxides could be cleaned by citric acid.

Different amounts of the reducing agent $NaBH_4$ were added into the precursor solution to investigate the effect on nanosolder particle size. The reaction took place with 1.5 times PVP addition and at 25°C. For

$NaBH_4/SnSO_4 = 1$, it is difficult to determine the particle size due to its large distribution range. Some nanosolders have high aspect ratio rather than being spherical. Based on results, increasing the amount of $NaBH_4$ addition resulted in the generation of nanosolders with narrow size distribution. Spherical nanosolders with diameters of 10 nm to 22 nm can be obtained with 4 times $NaBH_4$ addition. At low ratio of $NaBH_4/SnSO_4$, the reduction rate of the metallic ions is low and only a small amount of nuclei are generated at the nucleation step, leading to larger particles formed after the subsequent diffusional growth. On the contrary, as the concentration of $NaBH_4$ increases, more BH_4^- ions are available for transferring electrons to the metallic ions. As a result, a large number of nuclei are formed in the solution and act as self nucleation centers. The formation of this large number of nuclei consumes a large portion of the metallic ions in solution, which inhibits the growth of nanosolders, leading to the formation of spherical nanosolders with narrow size distribution [38].

Hsiao and Duh synthesized Sn-3.5Ag-*x*Cu (x = 0.2, 0.5, 1.0) nanoparticles by chemical precipitation with $NaBH_4$ [4]. The XRD patterns revealed that the Ag_3Sn was formed due to the alloying process. Besides, only Cu_6Sn_5 was formed when Cu concentration was as high as 1.0 wt% in the derived nanopowders. The formation of Ag_3Sn and Cu_6Sn_5 gave strong evidence that the nanoparticles were mixed homogeneously. From TEM observation, the isolated particles were close to spherical shape and the particle sizes of powders were about 5 nm. The field emission scanning electron microscopy morphology of Sn-Ag-Cu nanoparticles indicates that the major particle size of Sn-Ag-Cu nanoparticles is in the range of 40 nm.

Jiang et al. synthesized Sn-Ag-Cu alloy nanoparticles with various sizes [39]. It was found that the 10-13 nm (average diameter) Sn-Ag-Cu alloy nanoparticles have a low melting point at ~199°C, which will be compatible with the reflow temperature of the conventional eutectic micron sized Sn-Pb alloy particles. The as-synthesized Sn-Ag-Cu alloy nanoparticles were dispersed into an acidic type flux to form the nanosolder pastes. Their wetting properties on the cleaned copper surface were studied. It was found

that the nanoparticle pastes completely melted and wetted on the copper surface and the tin and copper IMCs formed. These low melting point Sn-Ag-Cu alloy nanoparticles could be used for low temperature lead-free interconnect applications.

At room temperature Sn-3.5Ag-0.5Cu nanoparticles were synthesized by chemical precipitation with $NaBH_4$ in aqueous solutions [40]. The results indicated that the primary particles after precipitation were $(Ag, Cu)_4Sn$, with a size of 4.9 nm. $(Ag, Cu)_4Sn$ was transformed into $(Ag, Cu)_3Sn$, when the total amount of Sn contributed from both $(Ag, Cu)_4Sn$ and Sn covering the $(Ag, Cu)_4Sn$ overtook that of $(Ag, Cu)_3Sn$. The final particle size of polycrystalline particles was 42.1 nm owing to the depletion of Sn atoms in the solution.

The polyol process is one of the chemical reduction methods. It has been proposed as a method for the preparation of finely divided powders of easily reducible metals, in which the metal salts are dissolved or suspended into the liquid polyols such as ethylene glycol, diethylene glycol or a mixture of both. The polyol acts as both the solvent for starting inorganic compounds and a reducing agent. PVP can be used as the protective agents for preventing nanoparticles from sintering, which covered the surface of silver nanoparticles and prevent the possibility of silver-silver particle bond formation [41].

A various size of Sn-Cu nanoparticles were synthesized by using a modified polyol process for low temperature electronic devices [42]. Monodispersive Sn-Cu nanoparticles with diameters of 21 nm, 18 nm and 14 nm were synthesized. The peak melting temperature of the Sn-0.7Cu bulk alloy was 230.6°C. The peak melting temperatures of the 21 nm, 18 nm and 14 nm Sn-0.7Cu nanoparticles were 212.9°C, 207.9°C and 205.2°C, respectively. These temperatures are 17.7°C, 22.7°C and 25.4°C lower than the corresponding temperatures of the Sn-0.7Cu bulk alloys. Another observable feature beside the melting temperature depression was the broadening of the melting temperature peak. This feature is more evident for smaller nanoparticles than for bulk alloys.

Nanocrystalline samples of pure Sn and of Sn-rich ternary Ni-Sb-Sn alloys, with compositions ranging from 80 to 97.5 at% Sn and a Ni to Sb molar ratio of 1 : 1, were synthesized by reduction of stoichiometric metal chloride solutions with $NaBH_4$ at 0°C in alkaline medium [43]. In the first step aqueous stock solutions of $SnCl_2$ (0.08 M), $SbCl_3$ (0.03 M), and $NiCl_2$ (0.06 M) were prepared by dissolving $SnCl_2{\cdot}2H_2O$ and $SbCl_3$ (99.99% purity) in diluted hydrochloric acid (5 M), and $NiCl_2.6H_2O$ (99.9985% purity) in distilled water. Appropriate volumes of the above metal chloride solutions were mixed together to make compositions with Sn contents varying from 80 to 97.5 at% and with a Ni to Sb molar ratio of 1:1. To the resulting solutions required amounts of a 1 M solution of tri-sodium citrate was added as chelating reagent. A 0.5 M $NaBH_4$ stock solution was prepared at a pH value of 14 from a 4.4 M $NaBH_4$ stable solution. The two separate aqueous solutions were cooled to 0°C in ice water before reaction. 40 mL of metal chloride solution was added drop wise within 10 min to 40 mL of the $NaBH_4$ solution under strong magnetic stirring. With continued addition, the color of the solution turned brown with formation of some bubbles which was followed by the appearance of some black suspensions. The mixed solutions were stirred for another 30 min, and for the entire period the reaction vessel was cooled in ice water. The resultant suspensions were separated by centrifuge and rinsed several times with distilled water and acetone. The precipitate was dried under vacuum at room.

The particle sizes of the obtained alloys were found to be in the range of 40-350 nm. A relative decrease in melting temperature of up to 15°C was observed for these alloys compared to a bulk sample.

The nanoscaled Sn-3.5Ag solder was prepared successfully by a supernatant process [44]. 9.65 g of Sn powder was weighed to mix 0.35 g of Ag powder in a sealed vacuum tube. Then the tube was placed in an oven and was heated at temperature 260°C for 2 h with intermittent shaking. The as-received alloy was immersed in the solvent, paraffin oil, and heated again at temperature 320°C for 10 h with a magnetic stirrer for blending the solution. To prevent the alloyed particles from agglomerating, the solution was quenched and the viscosity was raised by mixing with dry ice. Then the

supernatant, composed of Sn-3.5Ag particle and paraffin, was scooped up and blended with chloroform to dilute the paraffin.

It was found that the average diameter of the particle was 137 nm with a standard deviation of ± 5 nm. The eutectic element, Ag with a weight percentage of 3.5%, was found to be homogenous over all of the particles. It was found that the trace element, Ag was dissolved in the matrix, a tetragonal system, without an intermetallic phase.

Gao et al. [45] prepared nanoparticles with a consumable-electrode direct current arc (CDCA) technique. Nanoparticles were prepared from the master alloy with a recently developed consumable-electrode direct current arc (CDCA) technique as shown schematically in Figure 7 [45].

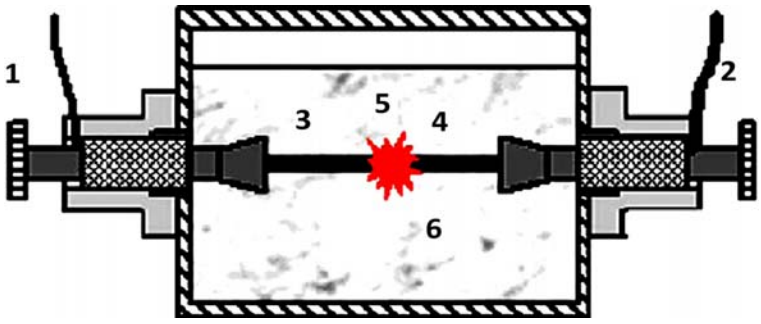

Figure 7. Schematic of the CDCA setup for nanoparticles preparation (1) cathode, (2) anode (connected to a high current and low voltage power source), (3) and (4) bulk alloy electrodes, (5) arc discharge taking place between the electrodes, and (6) dielectric coolant.

Liquid paraffin was chosen as a dielectric protection media. The anode and cathode, with a diameter of 6 mm, were made from the master alloy by means of a suction casting technique. The anode and the cathode electrodes were fixed inside the CDCA container and connected to a power supply. When the two electrodes get close enough, an arc discharge could be produced between them, causing a local melting and breakdown of the solder material into nanoparticles. The obtained particles were rinsed with chloroform for several times to remove the liquid paraffin. Furthermore, the rinsed particles were centrifugally separated at 4000 rpm for 45 min to

remove the possibly existed large particles. It was found that the size of most particles at 20 A arc current was in the range 15-60 nm with an average of about 30 nm. The melting peak of the aforementioned nanoparticles was shifted to lower temperatures and broadened. The peak onset temperature was decreased to about 197°C, 20°C lower than that of the bulk master alloy. Increasing the arc current to 50 A led to a significantly narrower size distribution of the nanoparticles. The particle size was concentrated in the range 25-42 nm, again with an average of about 30 nm. The melting onset temperature is lowered below 190°C and remained nearly unchanged even after repeated heating-cooling cycles. Due to the large specific surface area of the nanoparticles, it was hard to avoid oxidation during preparation, storage and the measurement.

The Sn-3.5Ag droplets in various sizes have been prepared by the consumable-electrode direct current arc technique [46]. The cooling rates of the droplets have been evaluated based on Newton's cooling law and it shows that the cooling rates of the droplets increase dramatically from 6.84×10^2 to 2.52×10^5 K/s as the droplet size decreases from 830 to 43 μm. The range of cooling rate is close to that of laser soldering (up to 10^4 K/s). It has been found that the β-Sn dendrites are refined as the cooling rate increase, and when the cooling rate is 1.30×10^5 K/s, which corresponding to the size scale smaller than 60 μm, the dendrites nearly disappear in the droplets. In addition, it has been observed that the high cooling rate could successfully avoid the precipitation of plate-like Ag_3Sn and promote the formation of nanoparticles which are desirable in practical application. These nanoparticles uniformly distribute in the Sn matrix and the average size of nanoparticles in different droplets is 46.4 nm (in 380-830 μm droplets), 57.2 nm (in 150-250μm droplets), 60.6nm (in 96-150μm droplets), 63.2nm (in 43-60μm droplets) and 65.3nm (in droplets of < 43μm), respectively. According to the dispersion-strengthening effect, the existence of nanoparticles would be beneficial to improve the mechanical property of the Sn-3.5Ag solder alloy.

The nanoparticles of Sn-3.0Ag-0.5Cu were manufactured using the self-

developed consumable-electrode direct current arc (CDCA) technique [47]. Two different protection dielectric media were used, namely liquid paraffin and triethanolamine. The electrodes manufactured from the master alloy by means of a suction casting technique had a circular cross section with a diameter of 6 mm. The anode and the cathode electrodes were fixed inside the CDCA container and externally connected to a power supply. When coming close enough, an arc discharge is produced between the electrodes, resulting in local melting and breakdown of the solder material into small nanoparticles. The discharge and solder alloy breakdown takes place inside the dielectric media. The manufactured nanoparticles were almost spherical in shape and the size distribution was between ≈ 10 nm and 100 nm.

The DSC results showed that the melting temperature of the nanoparticles was 213°C, which is approximately 10°C lower compared with that of the bulk alloy. No difference in morphology and melting temperature was found between the nanoparticles manufactured in liquid paraffin and with triethanolamine, meaning that both dielectric media are suitable to protect the nanoparticles from oxidation. The depression in melting temperature of the investigated SAC nanoparticles can be attributed to the large particle free energy caused by the size effect.

A low temperature chemical reduction method is employed to synthesize the Ag-Cu alloy nanoparticles for lead-free interconnects applications [48]. Figure 8 shows the XRD patterns of Ag-Cu alloy nanoparticles synthesized by chemical reduction reaction using $CuSO_4 + AgNO_3$ and $Cu(OAC)_2 + AgNO_3$, respectively. The crystallite size of Ag-Cu alloy size is found to be in the range of 13-16 nm for the sample prepared with $CuSO_4 + AgNO_3$ and 13-15 nm for the sample prepared with $Cu(OAC)_2 + AgNO_3$. Figure 9(a) shows the typical SEM image of the Ag-Cu alloy nanoparticles prepared from $CuSO_4 + AgNO_3$. The spherical alloy particles remain well separated, and the size distribution calculated from several SEM images indicates that the average particle diameter is in the range of (65 ± 5) nm. Figure 9(b) shows the typical SEM image of the Ag-Cu nanoalloys nanoparticles prepared from $Cu(OAC)_2 + AgNO_3$. The spherical alloy particles linked with each other, and the size distribution calculated from several SEM images indicates that the

average particle diameter is in the range of (50 ± 10) nm. In addition, few large particles of 100 nm were also found [48].

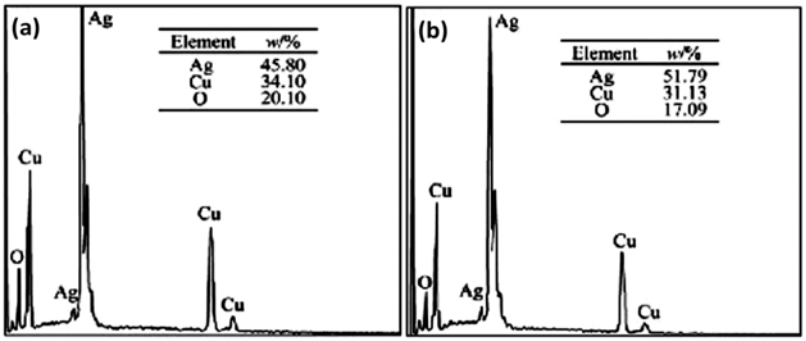

Figure 8. EDS profiles of Ag-Cu alloy nanoparticles synthesized from $CuSO_4 + AgNO_3$ (a) and $Cu(OAC)_2 + AgNO_3$ (b) [48].

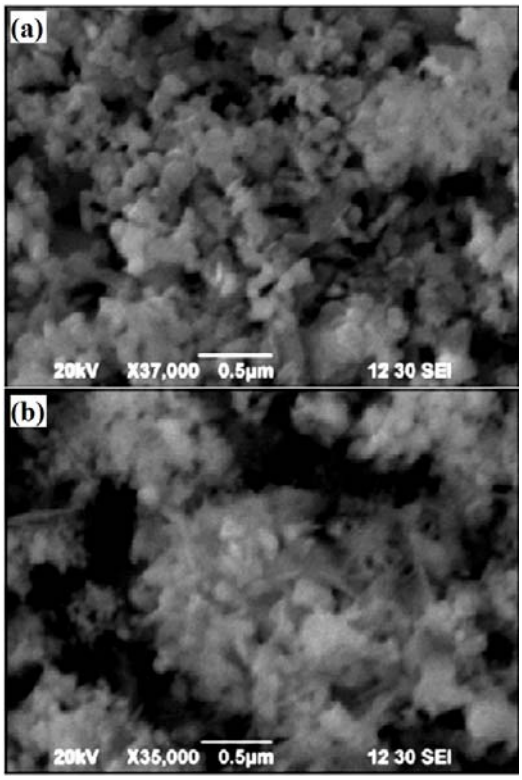

Figure 9. SEM images of Ag-Cu alloy nanoparticles synthesized from $CuSO_4 + AgNO_3$ (a) and $Cu(OAC)_2 + AgNO_3$ (b) [48].

For readers' convenience, the fundamentals, advantages/disadvantages of each method, and compositions of different nanomaterials produced in various studies are given in Table 4.

Table 4. Synthesis of different nanosolders produced in various studies

Materials	Method	Conditions	Results
Sn-Ag	Two fundamentally differing routes	**Route 1. In the first step**, 40 mL of silicone oil, 1 g of hydrazine hydrate, and 96.5 mg of 99.9% tin powder were mixed together in a 100 mL two necked flask equipped with stirring and refluxing equipment. The mixture was heated to ~240°C with vigorous stirring for 3 h for molecularization of metallic tin. **In the second step**, 3.5 mg of black resorcinol capped silver nanoparticles was added into the flask but at room temperature. Alternatively, oleic acid capped silver nanoparticles were used, which yield similar result. The reaction mixture containing molecularized tin and silver nanoparticles was then heated to ~240°C for 8 h reflux. The reaction mixture was cooled, and the suspended particles were centrifuged to obtain the black product. Finally, the black mass was washed thrice with petroleum ether (60-80) and three times with tetrahydrofuran (THF)	The particle size become quite smaller (~30 nm) than the particles obtained from Route 1. A sharp lowering of the melting point (~128°C) [12].

		and then dried under vacuum. The percent yield was 87%. **Route 2.** In this step, 20 mL of silicone oil, 20 mL of ethylene glycol, 96.5 mg of 99.9% Sn(II) acetate, 3.5 mg of 99.9% Ag(I) acetate, and 200 mg of NaOH were mixed in a 100 mL two necked flask. The mixture was then sonicated (~2 h) for homogeneous mixing. The mixture turned black. After that, the mixture was heated to ~240°C with vigorous stirring for 8 h for the preparation of Sn-Ag nanoalloy. Next, the reaction mixture was cooled, and the suspended particles were centrifuged to obtain the black product. Finally, the black mass was washed with petroleum ether (60-80) and THF. The product yield was 93%.	
Sn-3.5Ag (wt%)	Chemical reduction	- Using different amounts of reducing agent ($NaBH_4$) (0.01 - 1 g) [33] - 0.33 g of tin(II) 2-ethylhexanoate as precursor in the presence of 0, 0.1, 0.2 and 0.4 g surfactants were marked as Sn1, Sn2, Sn3 and Sn4, respectively. The melting temperatures of the Sn1, Sn2, Sn3 and Sn4 nanoparticles in diameter of 81, 40, 36 and 34 nm were 226.1, 221.8, 221.1 and	- The larger depression of the melting temperature of the nanoparticle with 50 nm was about 7°C [31]. The size of the nanoparticles ranged from 300 to 700 nm [33]. - The melting temperature of Sn-3.5Ag nanoparticles with average size of 30 nm was 210°C much

		219.5°C, and the corresponding latent heats of fusion were 35.9, 23.5, 20.1 and 15.6 J/g, respectively [35].	lower than that of bulk alloy [35].
	Supernatant process	9.65 g of Sn powder was weighed to mix 0.35 g of Ag powder in a sealed vacuum tube. Then the tube was placed in an oven and was heated at temperature 260°C for 2 h with intermittent shaking. The as-received alloy was immersed in the solvent, paraffin oil, and heated again at temperature 320°C for 10 h with a magnetic stirrer for blending the solution. To prevent the alloyed particles from agglomerating, the solution was quenched and the viscosity was raised by mixing with dry ice. Then the supernatant, composed of Sn-3.5Ag particle and paraffin, was scooped up and blended with chloroform to dilute the paraffin [44].	The average diameter of the particle was 137 nm [44].
Tin (Sn)	Chemical reduction	- 0.33 g of tin(II) 2-ethylhexanoate as precursor in the presence of 0, 0.1, 0.2 and 0.4 g surfactants were marked as Sn1, Sn2, Sn3 and Sn4, respectively. The melting temperatures of the Sn1, Sn2, Sn3 and Sn4 nanoparticles in diameter of 81, 40, 36 and	In the presence of 0, 0.1, 0.2 and 0.4 g surfactants were marked as Sn1, Sn2, Sn3 and Sn4, respectively. The melting temperatures of the Sn1, Sn2, Sn3 and Sn4 nanoparticles in diameter of 81, 40, 36 and 34 nm were 226.1,

		34 nm were 226.1, 221.8, 221.1 and 219.5°C, and the corresponding latent heats of fusion were 35.9, 23.5, 20.1 and 15.6 J/g, respectively [27]. - Using 2.1×10^{-4}mol tin(II) acetate as a precursor in the presence of 0.045 mol surfactants and 0.1 g sodium borohydride as reducing agents. Using 4.2×10^{-4}mol tin(II) acetate as a precursor in the presence of 0.045 mol surfactants. Using 1.1×10^{-3}mol tin(II) acetate as a precursor in the presence of 0.045 mol surfactants. Using 1.75×10^{-4}mol tin(II) acetate as a precursor in the presence of 0.045 mol surfactants [28].	221.8, 221.1 and 219.5°C, and the corresponding latent heats of fusion were 35.9, 23.5, 20.1 and 15.6 J/g, respectively [27]. - The average particle size calculated from the TEM picture was around 61 nm. The interplanar spacing was about 0.29 nm which corresponds to the orientation of (200) atomic planes of the tetragonal structure of Sn [28].
Sn-3.0Ag-0.5Cu		- Different amounts of tin(II) 2-ethylhexanoate were mixed into 60 mL anhydrous ethanol and the concentrations for SAC1, SAC2, SAC3, SAC4 were 0.0068, 0.0101, 0.0202 and 0.0271 mol/L, respectively. In a typical synthesis process, for example SAC1, 0.222 g surfactant was added into the solution and intensively stirred for about 2 h in atmospheric environment. Afterwards 0.0946 g reducing agent	The particle sizes of SAC1 and SAC2, whose solution concentrations were at relatively low level, were smaller than 50 nm and mainly concentrated in the range of 15-40 nm. In the case of higher reactant concentration, namely SAC3 and SAC4, the proportion of particles less than 50 nm was rapidly reduced to about 65% [29].

		was added into the homogeneous precursor solution and stirred for another 1 h till the end of the reaction [29]. - Authors mixed 0.3293 g tin(II) 2-ethylhexanoate, 0.0047 g silver nitrate, 0.0017 g copper(II) acetate monohydrate and 0.1110 g 1,10-phenanthroline into a 60 mL anhydrous ethanol solution. The solution was then stirred intensively for 2 h. Then 0.1892 g sodium borohydride was added into the solution and the reaction continued for 1 h at ambient temperature. Different amounts of surfactant, i.e., 0.1110 g, 0.4440 g, and 0.8880 g, were chosen to control the morphology and size distribution of the products [30].	The calorimetric onset melting temperature could be as low as 200°C, which was about 17°C lower than that of the bulk alloy (217°C). The particle size is smaller than 50 nm [30]. The melting temperature with average size of 30 nm was 201°C, much lower than that of bulk alloy [35]. - The particle size was smaller than 100 nm. The melting temperature was 214.7°C, 213.8°C, 213.5°C and 213.6°C lower than that 217.8°C of the bulk alloy. Undercooking was in the range of 82.0-88.5°C at different cooling rates [46]. - The nanosolder particle diameter was well controlled to the range of 10 nm to 22 nm, and the size-dependent melting point was depressed to 204.4°C [37]. - The 10-13 nm (average diameter) nanoparticles have a low melting point at ~199°C [39]. - The final particle size of polycrystalline particles was 42.1 nm

			owing to the depletion of Sn atoms in the solution [40].
Sn-3.5Ag-xZn (x = 0.5 to 3.5 wt%)	Chemical precipitation method was carried out by using $NaBH_4$ as a reducing agent and PVP as a stabilizer.	Tin sulphate ($SnSO_4$), silver nitrate ($AgNO_3$), zinc nitrate, $Zn(NO_3)_2$; sodium borohydride ($NaBH_4$) and PVP of molecular weight ~40,000 were used. Both $NaBH_4$ and PVP were dissolved in a beaker containing 200 ml of distilled water using a Teflon coated magnetic stirrer. The stoichiometric amounts of the salts, i.e. $SnSO_4$, $AgNO_3$ and $Zn(NO_3)_2$ were dissolved in aqueous solution as the metal precursors. The total weight of the Sn-Ag-Zn alloy was 2 g. Solutions of these metal precursors were rapidly added to $NaBH_4$, PVP, NaOH solution under constant stirring for 3-4 h. The stirring time was varied from 12 h to 48 h to ensure complete reduction. A black coloured precipitate was obtained after stirring for 12 h. The upper aqueous layer of the solution was removed and to the rest of the precipitated solid, 2 g of PVP dissolved in 200 mL of distilled water was added. Then the solution was stirred for 2 consecutive days. The	The isolated particles were spherical in shape and the particle size varied from 2 to 10 nm [36].

		black precipitate was washed several times with distilled water and filtered. The precipitate thus obtained was then dried in the oven maintained at 40°C for 12 h [36].	
Sn-3.5Ag-*x*Cu (*x* = 0.2, 0.5, 1.0)	Chemical precipitation with $NaBH_4$		The particle size is in the range of 40 nm. One endothermic peak at 215°C. Also, Sn-Ag-Cu nanopowders showed good wettability with contact angles less than 30° [38].
Sn-0.7Cu	Polyol process	Tin (II) acetate ($Sn(C_2H_3O_2)_2$) and copper(II) acetylacetonate ($Cu(C_5H_7O_2)_2$) were used as precursors of the Sn-Cu nanoparticles. The reducing agent, surface stabilizer, and solvent were $NaBH_4$ (99%, Sigma-Aldrich), poly(vinyl pyrrolidone) (PVP) (MW = 55000), and 1,5 pentanediol (96%), respectively. All chemicals were used as received without further processing or purification. All solutions were vacuumed and purged argon continuously during experiments to prevent from oxidations. This step was followed by various heating temperatures under argon in the presence of PVP [42].	The peak melting temperatures of the 21 nm, 18 nm and 14 nm Sn-0.7Cu nanoparticles were 212.9°C, 207.9°C and 205.2°C, respectively [42].

Ni-Sb-Sn	Prepared with compositions ranging from 80 to 97.5 at% Sn and a Ni to Sb molar ratio of 1 : 1, were synthesized by reduction of stoichiometric metal chloride solutions with $NaBH_4$ at 0°C in alkaline medium.	In the first step aqueous stock solutions of $SnCl_2$ (0.08 M), $SbCl_3$ (0.03 M), and $NiCl_2$ (0.06 M) were prepared by dissolving $SnCl_2{\cdot}2H_2O$ and $SbCl_3$ (99.99% purity) in diluted hydrochloric acid (5 M), and $NiCl_2{\cdot}6H_2O$ (99.9985% purity) in distilled water. Appropriate volumes of the above metal chloride solutions were mixed together to make compositions with Sn contents varying from 80 to 97.5 at% and with a Ni to Sb molar ratio of 1 : 1. To the resulting solutions required amounts of a 1 M solution of tri-sodium citrate was added as chelating reagent. A 0.5 M $NaBH_4$ stock solution was prepared at a pH value of 14 from a 4.4 M $NaBH_4$ stable solution. The two separate aqueous solutions were cooled to 0°C in ice water before reaction. 40 mL of metal chloride solution was added drop wise within 10 min to 40 mL of the $NaBH_4$ solution under strong magnetic stirring. With continued addition, the color of the solution turned brown with formation of some bubbles which was followed by the appearance	The particle sizes were found to be in the range of 40-350 nm [43].

		of some black suspensions. The mixed solutions were stirred for another 30 min, and for the entire period the reaction vessel was cooled in ice water. The resultant suspensions were separated by centrifuge and rinsed several times with distilled water and acetone. The precipitate was dried under vacuum at room [43].	

8. Conclusions

Nanoparticles show different properties from bulk materials because of their large surface area to volume ratio and quantum size effect. Bimetallic alloy nanoparticles are such a kind of materials with special properties that are different from either constituent in relation to their optical, catalytic and electronic properties.

Two kinds of methods have been developed to synthesize bimetallic alloy nanoparticles. One is called “bottom-up” method, the most studied chemical reduction technique; the other one is the physical method called “top-down” approach. The chemical reduction method for the preparation of bimetallic nanoparticles can be divided into two groups: one is the co-reduction of two different kinds of metal precursor salts. The other one is successive reduction of two metal salts, which is usually carried out to prepare a core-shell structure of bimetallic nanoparticles. Many researches on size or shape dependent properties for nanocrystals and their synthesis methodology have been reported, where interesting and exotic phenomenon were observed. Therefore, a discovery for a certain structure or form that has not been seen before, can open a new area of science, research or applications.

References

[1] C. J. Murphy, T. K. Sau, A. M. Gole, C. J. Orendorff, J. Gao, L. Gou, S. E. Hunyadi and T. Li, J. Phys. Chem. B 109 (2005), 13857.

[2] Y. Xia, P. Yang, Y. Sun, Y. Wu, B. Mayers, B. Gates, Y. Yin, F. Kim and H. Yan, Adv. Mater. 5 (2003), 353.

[3] Z. L. Wang, J. Phys.: Condens. Matter 16 (2004), R829.

[4] L. Y. Hsiao and J. G. Duh, J. Electrochem. Soc. 152 (2005), J105.

[5] A. E. Hammad, Mater. Des. 50 (2013), 108.

[6] K. Zeng and K. N. Tu, J. Mater. Sci. Eng. R 38 (2002), 55.

[7] M. Abtew and G. Selvaduary, J. Mater. Sci. Eng. R 27 (2000), 95.

[8] H. Jiang, K. Moon and C. P. Wong, Microelectron. Reliab. 53 (2013), 1968.

[9] S. Chantaramanee, S. Wisutmethangoon, L. Sikong and T. Plookphol, J. Mater. Sci.: Mater. Electron. 24 (2013), 3707.

[10] A. K. Gain and Y. C. Chan, Intermetallics 29 (2012), 48.

[11] V. L. Niranjani, B. S. S. Chandra Rao, Rajdeep Sarkar and S. V. Kamat, J. Alloys Compd. 542 (2012), 136.

[12] S. Pande, A. K. Sarkar, M. Basu, S. Jana, A. K. Sinha, S. Sarkar, M. Pradhan, S. Saha, A. Pal and T. Pal, Langmuir 24 (2008), 8991.

[13] H. Jiang, K.-S. Moon and C. P. Wong, Synthesis of Ag-Cu alloy nanoparticles for lead-free interconnect materials, 10th International Symposium on Advanced Packaging Materials: Processes, Properties and Interfaces, March 16-18, 2005, Irvine, CA.

[14] H. Jiang, K.-S. Moon, H. Dong, F. Hua and C. P. Wong, Chem. Phys. Lett. 429 (2006), 492.

[15] Y. J. Tian, Y. L. Zhang, Q. Yu, X. Z. Wang, Z. Hu, Y. F. Zhang and K. C. Xie, Catal. Today 89 (2004), 233.

[16] J. Zhu, M. Yudasaka and S. Iijima, Chem. Phys. Lett. 380 (2003), 496.

[17] T. Tsuji, Y. Tsuboi, N. Kitamura and M. Tsuji, Appl. Surf. Sci. 229 (2004), 365.

[18] T. Hirose, T. Omatsu, M. Sugiyama, S. Inazawa, A. Takami, M. Tateda and S. Koda, Jpn. J. Appl. Phys., Part 1 (42) (2003), 1288.

[19] K. D. Kim, S. H. Kim and H. T. Kim, J. Ind. Eng. Chem. (Seoul, Repub. Korea) 10 (2004), 906.

[20] M. Ojeda, S. Rojas, M. Boutonnet, F. J. Perez-Alonso, F. J. Garcia-Garcia and J. L. G. Fierro, Appl. Catal. A 274 (2004), 33.

[21] S. Karmakar, S. Taran and B. K. Chaudhuri, Phys. Status Solidi B 241 (2004), 3563-3571.

[22] M. Thiruchitrambalam, V. R. Palkar and V. Gopinathan, Mater. Lett. 58 (2004), 3063.

[23] K. S. Chou and C. Y. Ren, Mater. Chem. Phys. 64 (2000), 241.

[24] K. D. Kim, D. N. Han and H. T. Kim, Chem. Eng. J. 104 (2004), 55.

[25] H. S. Nalwa, Handbook of Nanostructured Materials and Nanotechnology, Vol. 1, Chap. 1, Academic Press, San Diego, CA, 2000.

[26] W. Zhang, B. Zhao, C. Zou, Q. Zhai, Y. Gao and S. F. A. Acquah, J. Nanomaterials 2013 (2013), Article ID 193725, 9 pp. http://dx.doi.org/10.1155/2013/193725.

[27] C. Zou, Y. Gao, B. Yang and Q. Zhai, Trans. Nonferrous Met. Soc. China 20 (2010), 248.

[28] H. Jiang, K. Moon, H. Dong, F. Hua and C. P. Wong, Chem. Phys. Lett. 429 (2006), 492.

[29] W. Zhang, B. Zhao, C. Zou, Q. Zhai and Y. Gao, Trans. Nonferrous Met. Soc. China 23 (2013), 1668.

[30] C. Zou, G. B. Yang and Q. Zhai, J. Mater. Sci.: Mater. Electron. 23 (2012), 2.

[31] C. Zou, Y. Gao, B. Yang and Q. Zhai, J. Mater. Sci.: Mater. Electron. 21 (2010), 868.

[32] Y. H. Jo, I. Jung, N. R. Kim and H. M. Lee, J. Nanopart, Res. 14(1) (2012), 782.

[33] H. J. Pan, C. Y. Lin, U. S. Mohanty and J. H. Chou, Mater. Sci. Appl. 2 (2011), 1480.

[34] H. Jiang, K. Moon, F. Hua and C. P. Wong, Chem. Mater. 19 (2007), 4482.

[35] C. D. Zou, Fundamental research on the melting temperature depression of the Sn based lead-free solder alloy via size effect of nanoparticles (Shanghai, Shanghai University, Steel Alloy Profession, 2010).

[36] C. Y. Lin, U. S. Mohanty and J. H. Chou, J. Alloys Compd. 472 (2009), 281.

[37] C. Zou, Y. Gao, B. Yang and Q. Zhai, Mater. Character. 61 (2010), 474.

[38] K. C. Yung, C. M. T. Law, C. P. Lee, B. Cheung and T. M. Yue, J. Electron. Mater. 41 (2012), 313.

[39] H. Jiang, K. Moon and C. P. Wong, Electronic Components and Technology Conference 1400, 2008.

[40] L. Y. Hsiao and J. G. Duh, J. Electron. Mater. 35 (2006), 1755.

[41] G. Carotenuto, G. P. Pepe and L. Nicolais, Eur. Phys. J. B 16 (2000), 11.

[42] Y. H. Jo, J. C. Park, J. U. Bang, H. Song and H. M. Lee, J. Nanosci. Nanotech. 11 (2011), 1037.

[43] R. Mishra, A. Zemanova, A. Kroupa, H. Flandorfer and H. Ipser, J. Alloys Compd. 513 (2012), 224.

[44] C. Y. Lin, J. H. Chou, Y. G. Lee and U. S. Mohanty, J. Alloys Compd. 470 (2009), 328.

[45] Y. Gao, C. Zou, B. Yang, Q. Zhai, J. Liu, E. Zhuravlev and C. Schick, J. Alloys Compds. 484 (2009), 777.

[46] J. Zhao, Y. Gao, W. Zhang, T. Song, Q. Zhai and J. Mater. Sci: Mater. Electron. 23 (2012), 2221.

[47] C. Zou, Y. Gao, B. Yang, X. Xia, Q. Zhai, C. Andersson and J. Liu, J. Electron. Mater. 38 (2009), 351.

[48] W. Bhagathsingh and A. Samson Nesaraj, Trans. Nonferrous Met. Soc. China 23 (2013), 128.